

Crystal Structure Analysis of Synthetic Fluorophlogopite

JAMES W. McCauley¹, R. E. NEWNHAM, AND G. V. GIBBS²

Materials Research Laboratory, The Pennsylvania State University,
University Park, Pennsylvania 16802

Abstract

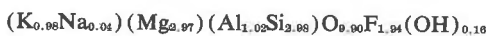
The crystal structure of synthetic 1M-fluorophlogopite has been determined from single-crystal diffractometer data and refined to a weighted R-factor of 6.1 percent by least-squares methods. Fluorophlogopite, $\text{KMg}_3\text{AlSi}_2\text{O}_{10}\text{F}_2$ possesses monoclinic space group symmetry $C2/m$ with $a = 5.308(2)$, $b = 9.183(3)$, and $c = 10.139(1)\text{\AA}$, $\beta = 100.07(2)^\circ$, and $Z = 2$. Various tests failed to reveal any significant long-range ordering of aluminum and silicon in the tetrahedral sites. Average bond lengths are as follows: (Al,Si)—O 1.642, Mg—(O,F) 2.063, inner K—O 3.006, outer K—O 3.273\AA. The tetrahedral rotation angle α is 5.9° .

Introduction

The basic structure of mica has been known for over forty years (Pauling, 1930), but accurate crystallographic data for different varieties have been obtained only within the last decade. Many mica structures, especially synthetic fluorine micas and micas with large divalent interlayer cations, remain unrefined. Precise refinements extend the crystal chemistry of mica, elucidating the structural origin of the physical properties and the various stacking arrangements which result in stacking faults, twins, and polytypes. The data are also useful in developing formulae to predict the structural features of other micas (Donnay, Donnay, and Takeda, 1964; McCauley and Newnham, 1971).

Experimental

A crystal was selected from a batch synthesized at the Electrotechnical Laboratory of the Bureau of Mines at Norris, Tennessee. H. R. Shell and R. L. Craig (Bureau of Mines, Norris, Tennessee) and C. O. Ingamels (Mineral Constitution Laboratory, The Pennsylvania State University) independently determined the following bulk chemical composition:



The homogeneity of the batch was confirmed by electron microprobe analyses of several individual crystals. Lattice parameters determined from powder data for this batch

were reported previously by Bloss, Gibbs and Cummings (1963): $a = 5.308(2)$, $b = 9.183(3)$, $c = 10.139(1)\text{\AA}$, $\beta = 100.07(2)^\circ$. The measured density of 2.882 g/cm^3 is in good agreement with 2.870 g/cm^3 , the value calculated assuming $Z = 2$.

All of the crystals examined by Weissenberg and precession methods exhibited undesirable characteristics such as diffuse streaks, twinning, and complex polytypism. A specimen measuring approximately $0.056 \times 0.089 \times 0.32\text{ mm}$ was selected for analysis since it was more nearly perfect than the others. Even this crystal showed faint extra spots and diffuse streaks on long-exposure Weissenberg photographs. The spots occurred at one-third the distance between major reflections along $0kl$ festoons, where $k \neq 3n$, with every third spot missing. No extraneous reflections were found in $h0l$ photographs. Sadanaga and Takeuchi (1961) describe this case as a polysynthetically twinned crystal with the festoons in question as twin rows; this situation corresponds to a 120° alternating twin type. Since, as estimated from photographic intensity data, the smaller twin element constituted only about 5 percent of the total crystal, it only slightly affected a small number of reflections of the type $k = 0 \pmod{3}$, and the crystal was considered acceptable for structure refinement. Faint diffuse streaks were observed on $0kl$ photographs when $k \neq 3n$, but not on $h0l$ photographs. This type of stacking disorder is symbolized as $1M_r - n(120)$ (Ross *et al.*, 1966), indicative of random stacking faults with $\pm 120^\circ$ rotations of the mica layers about c^* . Both the stacking faults and the twinning are controlled by rotations of 120° about c^* .

Intensities of 1,546 reflections were measured from eight layers about the a axis using Nb-filtered $\text{MoK}\alpha$ radiation and an equi-inclination Weissenberg diffractometer; only reflections with $\sin \theta$ less than 0.5 were measured. Diffracted radiation was recorded with a scintillation counter and pulse height analyzer system. Each reflection was scanned symmetrically through ϕ for 100 seconds at a scanning rate of 1.8° per minute; the background was obtained by counting for 20 seconds at two positions $1.5^\circ \phi$ removed from the center of the peak. The integrated intensity was obtained by

¹ Present address: Army Material and Mechanics Research Center, Watertown, Massachusetts 02172.

² Present address: Department of Geological Sciences, Virginia Polytechnic Institute and State University, Blacksburg, Virginia 24061.

subtracting the adjusted background from the total count. The 1,546 intensities were reduced to 535 non-equivalent values by averaging symmetry-equivalent reflections and excluding 380 below the observational limit of the detector or where $F \leq \sigma(F)$. Each reflection was assigned a weight ($w = 1/\sigma^2$) consistent with the standard deviation estimated by the range-estimate technique (Ibers, 1956). This technique has theoretical justification (Abrahams, 1964) and has been tested experimentally (McCauley and Gibbs, 1967). Intensities were corrected for Lorentz-polarization effects, but absorption corrections were unnecessary because of the negligible difference in the maximum (1.35) and minimum (1.06) transmission factors ($\mu = 12.85 \text{ cm}^{-1}$).

The diffraction symbol, $1\ 2/m\ 1\ C\ \dots$, is consistent with monoclinic space groups $C2/m$, $C2$ and Cm . Examination of the intensity data utilizing several $N(Z)$ tests (Bailey, 1966) failed to provide a definite answer with regard to the presence of a center of symmetry, indicating that all three space groups should be tested in the ensuing refinements. The space group assignment is intimately related to order-disorder. Several arrangements for aluminum-silicon ordering in the two tetrahedral sheets are illustrated in Figure 1. Only the C -centered patterns are possible since no reflections violating the C -centering condition were observed.

Structure Refinement

The atomic coordinates of ferriphlogopite (Steinfink, 1962) were used as starting parameters in refining fluorophlogopite. Scattering factors for K^+ ,

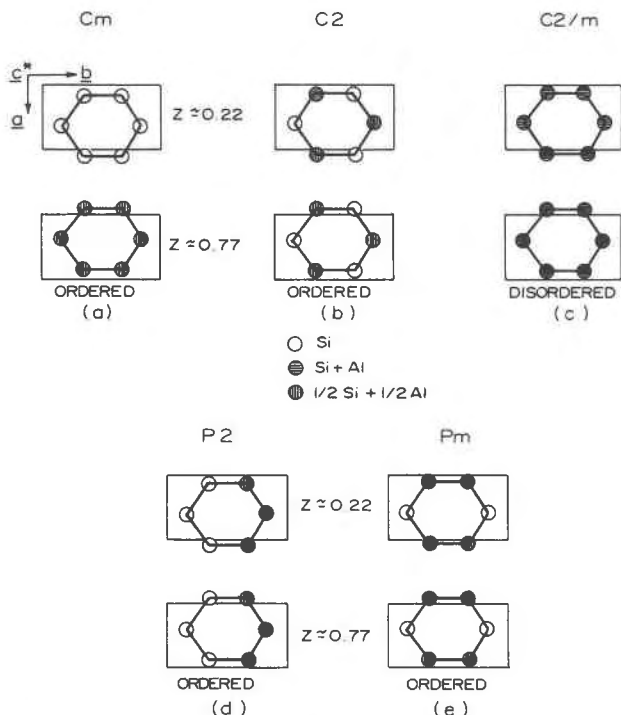


FIG. 1. Schematic diagrams of aluminum-silicon ordering in the two tetrahedral sheets for $AlSi_2$ -type micas.

TABLE 1. Results of Refinements in $C2/m$, $C2$, and Cm

	$C2/m$	$C2$	Cm
<u>Isotropic Refinements</u>			
R	8.8%	6.7%	15.3%
wR	12.3%	7.4%	16.1%
Variable parameters	30	47	50
$ F_o _s$	520	520	520
<u>Anisotropic Refinements</u>			
R	6.3%	6.3%	
wR	6.1%	6.1%	
Variable parameters	60	99	

Mg^{2+} , Al^{3+} , and Si^{4+} were taken from the International Tables for X-Ray Crystallography, Vol. III, and the values for O^{2-} from Tokonami (1965). The real part of the dispersion correction was included in the calculation. Both isotropic and anisotropic temperature factors were utilized in the least squares analyses with the results shown in Table 1.

Computations were carried out in all three space groups using the ORFLS program (Busing, Martin, and Levy, 1962). Least squares refinement in $C2$ and Cm required special techniques because of large correlations between atomic parameters related by symmetry in $C2/m$. The high correlation effects were suppressed by independently refining the parameters of symmetry-related atoms. Cell origins in the $C2$ and Cm refinements were established by fixing the interlayer cation K at (0,0,0). Utilizing Hamilton's (1965) criteria, the anisotropic refinement in $C2/m$ is superior to the others and is accepted as the valid refinement. Moreover, the $C2$ and Cm refinements did not yield acceptable results for some of the refined parameters. For example, in $C2$ the y parameter of F never converged, and the β_{ij} values obtained for O_1 , O_2 , O_3 , and M_3 were not physically meaningful. As a check on Al-Si order, T-O (tetrahedral cation-oxygen) bond lengths were computed for the tetrahedra in $C2/m$ and $C2$ using the final coordinates. $C2/m$ gave a mean T-O distance of 1.642(2)Å. The two crystallographically-independent tetrahedra in $C2$ refined to 1.646(6) and 1.639(6)Å distances which are not significantly different.

Final agreement factors for $C2/m$ refinement are as follows: unweighted $R = 6.3$ percent, weighted $R = 6.1$ percent, and the standard deviation of an

TABLE 2. Final Atomic Coordinates, Anisotropic Temperature Factors, and Equivalent Isotropic Temperature Factor for Synthetic 1*M*-Fluorophlogopite, Refined in Space Group *C2/m**

	K	M ₁	M ₂	T	O ₁	O ₂	O ₃	F
Equipoint	2a	2d	4h	8j	8j	4i	8j	4i
x	0.0	0.0	0.0	0.5751(3)	0.8208(7)	0.5274(9)	0.6291(5)	0.1327(6)
y	0.0	0.5	0.8306(2)	0.1663(1)	0.2347(4)	0.0	0.1661(4)	0.0
z	0.0	0.5	0.5	0.2245(1)	0.1682(4)	0.1678(6)	0.3896(3)	0.4017(4)
β ₁₁	0.0269(13)	0.0073(13)	0.0056(9)	0.0070(6)	0.0116(13)	0.0174(22)	0.0062(12)	0.0068(14)
β ₂₂	0.0075(4)	0.0011(3)	0.0021(2)	0.0018(1)	0.0076(6)	0.0039(6)	0.0018(3)	0.0021(4)
β ₃₃	0.0052(3)	0.0005(3)	0.0014(2)	0.0023(1)	0.0022(4)	0.0021(5)	0.0014(3)	0.0032(5)
β ₁₂	0.0	0.0	0.0	0.00001(20)	-0.0036(6)	0.0	0.0008(5)	0.0
β ₁₃	0.0016(4)	0.0001(4)	0.0012(3)	0.0006(2)	0.00001(53)	-0.0001(8)	0.0009(5)	0.0010(6)
β ₂₃	0.0	0.0	0.0	0.0002(1)	-0.0010(3)	0.0	-0.0002(3)	0.0
Equivalent B	2.52(8)	0.47(7)	0.61(5)	0.76(3)	1.59(10)	1.38(13)	0.60(8)	0.91(10)

* Standard errors associated with the last digit are given in parentheses

observation of unit weight is 0.3724. Difference Fourier maps calculated using the F_c values from the *C2/m* analysis showed no significant accumulation of error at any point within the unit cell. Table 2 lists the refined values of the atomic positions and temperature factors, together with their standard errors. Seven scale factors were also refined in the calculations. The structure factors calculated from the refined values in Table 2 and observed absolute structure amplitudes are listed in Table 3.³

Discussion of the Refined Structure

Figure 2 shows a slightly idealized drawing of fluorophlogopite projected along *b*, the 2-fold axis. Figures 3-5 are illustrations of the interlayer, tetrahedral and octahedral sheets, respectively. In the figures the following notation is used: the first subscript corresponds to the atom notation in Table 2; the second subscript (or the first when Table 2 does not require one) signifies one of the 8 equivalent positions. Interatomic distances are listed in Table 4.

Fluorophlogopite differs only slightly from the ideal mica structure first reported by Pauling (1930) and by Jackson and West (1930). The ditrigonal distortion of the tetrahedral layer is unusually small ($\alpha = 5.88^\circ$) consistent with the small difference (0.27Å) between the inner and outer potassium-oxygen distances (McCauley and Newnham, 1971).

Radoslovich (1959) has pointed out that mica polytypes are formed by the rotation of identical

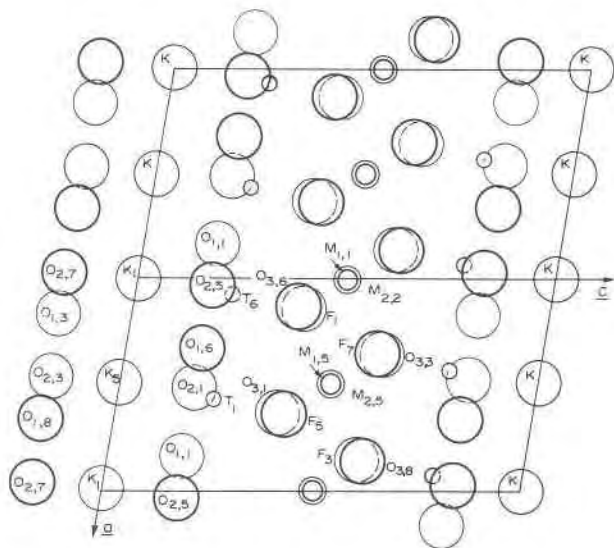


FIG. 2. Slightly schematic *b* axis view of fluorophlogopite, from $y = 0$ to $y = 1/2$.

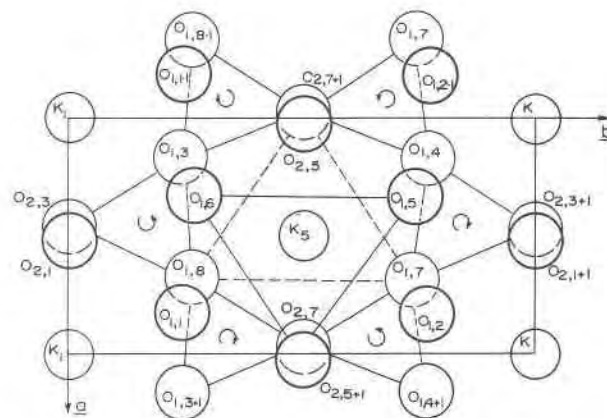


FIG. 3. A view of the interlayer cations and tetrahedral sheet anions perpendicular to (001). Dark oxygens are above K, light ones are below K.

³ To obtain a copy of Table 3, order NAPS Document 02027 from Microfiche Publications, Division of Microfiche Systems Corporation, 305 East 46th Street, New York, N. Y. 10017. Please remit in advance \$1.50 for microfiche or \$5.00 for photocopies. Please check the latest issue of this journal for the current address and prices.

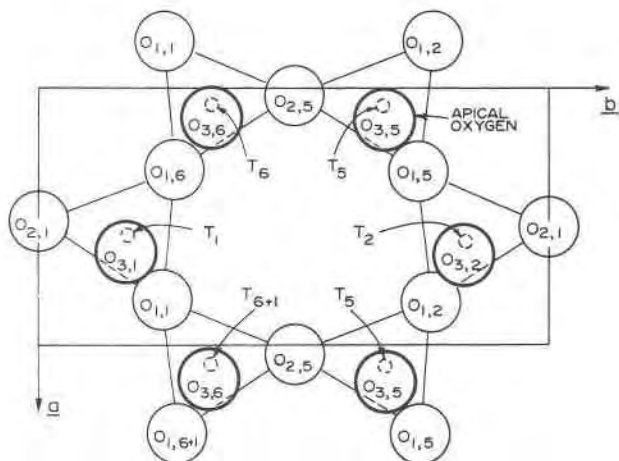


FIG. 4. Tetrahedral sheet of fluorophlogopite perpendicular to (001). Dark oxygens are apical oxygens above the basal plane.

layers, and that the ditrigonal basal-plane symmetry favors 120° rotations of successive layers. The vast majority of observed mica polytypes and twins are characterized by 120° stacking rotations. Only the $2M_2$ polytype of lepidolite exhibits a 60° change in stagger direction. Takeda and Burnham (1969) show that α is only 3° for fluor-polyolithionite, accounting for the occurrence of the $2M_2$ polytype in this group of micas. These results suggest that the maximum basal plane distortion compatible with $\pm 60^\circ$ or 180° rotations of successive layers lies between 3° and 6° , the values of α found in $2M_2$ fluor-polyolithionite and 1M-fluorophlogopite.

The substitution of F for OH in phlogopite has a marked effect on the thermal stability, hardness and

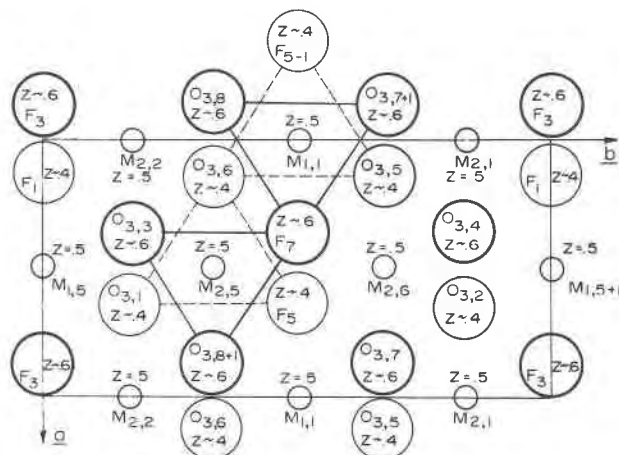


FIG. 5. Octahedral sheet of fluorophlogopite perpendicular to (001). Relative height of atoms are designated by z .

TABLE 4. Bond Lengths for 1M-Fluorophlogopite*

Bond	Multiplicity & length	Bond	Multiplicity & length
$K_5-O_{2,5}$	{2} 3.268(5)Å	$M_{1,1}-O_{3,5}$	{4} 2.078(3)Å
$K_5-O_{1,1}$	{4} 3.276(4)	$M_{1,1}-F_5$	{2} 2.029(3)
Mean	3.273(3)	Mean	2.062(2)
$K_5-O_{1,6}$	{4} 3.004(4)	$M_{2,5}-O_{3,1}$	{2} 2.068(4)
$K_5-O_{2,5+1}$	{2} 3.011(5)	$M_{2,5}-O_{3,6}$	{2} 2.088(3)
Mean	3.006(3)	$M_{2,5}-F_5$	{2} 2.038(3)
$T_1-O_{1,1}$	{1} 1.637(4)	Mean	2.065(2)
$T_1-O_{2,1}$	{1} 1.636(2)		
$T_1-O_{1,6}$	{1} 1.645(4)		
$T_1-O_{3,1}$	{1} 1.648(3)		
Mean	1.642(2)		

* The number of symmetrically equivalent distances is given in braces, and the estimated standard deviation error in parentheses.

resistance to chemical attack. The structural origin of these differences is not as yet clearly understood. It has been previously established that the substitution of F for OH in phlogopite decreases the c dimension (Noda and Roy, 1956; Noda and Ushio, 1964), whereas the same substitution in muscovite has no effect on the cell size (Yoder and Eugster, 1955). Hardness measurements (Bloss *et al.*, 1959), polarized infrared spectra (Bassett, 1960; Vedder and McDonald, 1963), and neutron inelastic scattering data (Naumann *et al.*, 1964) suggested that the hydroxyl group is oriented perpendicular to the octahedral sheet in phlogopite, rather than the almost parallel orientation found in muscovite. Neutron diffraction experiments on muscovite (Rothbauer, 1971) verified the proton position in the oxygen layer, confirming the spectroscopic work. The parallel and perpendicular positions can be explained in terms of the crystal structures. The hydroxyl ion is coordinated to three cations in trioctahedral micas, and to two cations in dioctahedral micas. In the trioctahedral group, the proton is repelled away from the octahedral layer toward the interlayer region, whereas in dioctahedral micas the proton moves toward the vacant octahedral site (Bloss *et al.*, 1959; Takeuchi, 1964). As shown in Figure 2, the fluorine atom in fluorophlogopite is situated directly above the interlayer potassium ion at a distance of 4.01Å. In hydroxyphlogopite, the fluorine ion is replaced by hydroxyl, with the OH group pointing toward the interlayer cation, resulting in coulomb repulsion between K^+ and H^+ , and increasing the interlayer separation from 3.36 to 3.62Å. The effect is less important in muscovite because the proton is located in the octahedral layer, about 1 Å further away from the interlayer cation. Therefore, substitution of

F for OH in muscovite does not alter the coulombic forces on the interlayer cation.

Since bond strength is inversely proportional to interatomic distance, interlayer bonds in K-micas are strongest in fluorophlogopite, somewhat weaker in muscovite, and appreciably weaker in hydroxyphlogopite. Physical and chemical property data reflect these deductions. The preceding discussion points out the importance of the interaction between the interlayer cation and the univalent anion in the octahedral sheet. Takeda and Burnham (1969) have emphasized the importance of this interaction in controlling polytypism in micas.

Further evidence of the regularity of the tetrahedral sheet in fluorophlogopite is the small corrugation of the basal oxygen layer, 0.004 Å, a value which does not differ significantly from zero. Except for a slight elongation along c^* , individual tetrahedra are also very regular. The four T -O bond lengths (Table 4) range between 1.637 and 1.648 Å, with a mean 1.642 Å. The longest distance is to the apical oxygen shared with the octahedral sheet. Oxygen-oxygen distances show a similar effect; those in the basal plane (2.658-2.673 Å) are slightly shorter than those from base to apex (2.692-2.696). The thickness of the tetrahedral layer is 2.21 Å. All angles are within 1° of the ideal values; tetrahedral face angles (O-O-O) range from 59.1 to 60.5°, and O- T -O bond angles lie between 108.6 and 110.3°.

In the octahedral sheet, the two independent octahedra are geometrically identical, as expected. Bond lengths (Table 4) are very similar, with Mg-O distances 2.068-2.088 Å and slightly smaller Mg-F distances, 2.029-2.038 Å. Shared edges are appreciably shorter than unshared edges because of cation-cation repulsion, flattening the octahedral sheet to a thickness of 2.124 Å. Oxygen-oxygen and oxygen-fluorine distances along unshared edges are very regular (3.050-3.069 Å), but shared edges fall into three groups: O-O 2.822-2.835, O-F 2.733, F-F 2.635 Å. Apparently there is less repulsion between univalent fluorines than between divalent oxygens. Bond angles across unshared edges are tightly grouped and longer (94.4-96.7°) than those across shared octahedron edges (80.5-86.0°).

Temperature factors (Table 2) provide a valuable source of information concerning vibrational and spatial disorder. They are, however, extremely sensitive to systematic errors in intensity measurement so that care must be exercised in their interpretation.

Potassium has the largest thermal vibration ampli-

tude of all the ions in fluorophlogopite. The temperature factor for the loosely-bonded K^+ ion is 2.5 \AA^2 , considerably larger than the values for T (0.76), M_1 (0.47) and M_2 (0.60). Basal oxygens O_1 and O_2 have higher temperature factors than F and O_3 , the apex oxygen. The isotropic B values for O_1 , O_2 , O_3 and F are 1.6, 1.4, 0.6 and 0.9 \AA^2 , respectively. Burnham (1965) has shown that in well-refined silicate structures the magnitude of the isotropic temperature factor of oxygen is related to the number of coordinating cations; two coordinated oxygen ions exhibit larger B values than three or four coordinated ones. The apical oxygen O_3 in fluorophlogopite is coordinated to four cations—three Mg ions and one tetrahedral cation. Bond lengths from O_3 to the coordinating cations are consistent with the ionic radii. The basal oxygen ions, O_1 and O_2 , are also coordinated to four cations, but the outer K-O bond lengths are appreciably larger than what is expected for a rigid coordination sphere. This implies that O_1 and O_2 are only weakly bonded to the potassium ions, but strongly coordinated to the tetrahedral cations. The B values of O_1 and O_2 are consistent with a coordination that is smaller than the rigid four-fold coordination of O_3 . In other words, the thermal motions of the basal oxygens are less restricted by cations than the apex oxygen. Fluorine is coordinated to three magnesium ions and has an intermediate-size temperature factor.

Positional disorder may also contribute to the higher temperature factors of O_1 , O_2 and the tetrahedral cations. Since Al is a larger ion than Si, spatial considerations dictate that O_1 must be further away from Al than Si, thus occupying two slightly different positions, causing an apparent thermal vibration which may be anisotropic. The largest vibration of both O_1 and O_2 is in the a b plane, almost perpendicular to c^* , as expected. The apical oxygen O_3 does not exhibit this kind of anisotropy because its movement is restricted by neighboring Mg ions.

Acknowledgment

This study was supported by the Army Materials and Mechanics Research Center under Contract No. DA-19-0660 AMC-325(X).

References

- ABRAHAMS, S. C. (1964) Estimation of error in the measured structure factor. *Acta Crystallogr.* **17**, 1327-1328.
- BAILEY, S. W. (1966) The status of clay mineral structures. *Proc. Nat. Conf. Clays Clay Mineral.* **14**, 1-23.
- BASSETT, W. A. (1960) Role of hydroxyl orientation in mica alteration. *Bull. Geol. Soc. Amer.* **71**, 449-456.

- BLOSS, F. D., E. SHEKARCHI, AND H. R. SHELL (1959) Hardness of synthetic and natural micas. *Amer. Mineral.* **44**, 33–48.
- BLOSS, F. D., G. V. GIBBS, AND D. CUMMINGS (1963) Polymorphism and twinning in synthetic fluorophlogopite. *J. Geol.* **71**, 537–547.
- BURNHAM, C. W. (1965) Temperature parameters of silicate crystal structures. *Amer. Mineral.* **50**, 282.
- BUSING, W. R., K. O. MARTIN, AND H. A. LEVY (1962) ORFLS, a Fortran crystallographic least-squares refinement program. *U.S. Nat. Tech. Infor. Serv.*, **ORNL-TM-305**.
- DONNAY, G., J. D. H. DONNAY, AND H. TAKEDA (1964) Trioctahedral one-layer micas. II. Prediction of the structure from composition and cell dimensions. *Acta Crystallogr.* **17**, 1374–1381.
- HAMILTON, W. C. (1965) Significance tests on the crystallographic *R* factor. *Acta Crystallogr.* **18**, 502–510.
- IBERS, J. A. (1956) Estimates of the standard deviations of the observed structure factors and of the electron density from intensity data. *Acta Crystallogr.* **9**, 652–654.
- JACKSON, W. W., AND J. WEST (1930) The crystal structure of muscovite. *Z. Kristallogr.* **76**, 211–227.
- MACGILLAVRY, C. H., AND G. D. RIECK, Eds. (1962) *International Tables for X-ray Crystallography, Vol. III*. The Kynoch Press, Birmingham.
- McCAULEY, J. W., AND G. V. GIBBS (1969) Significance of weighting schemes in an anisotropic least squares refinement of a ruby. *Nat. Bur. Stand. Spec. Publ.* **301**, 277–282.
- , AND R. E. NEWNHAM (1971) Origin and prediction of ditrigonal distortions in micas. *Amer. Mineral.* **56**, 1626–1638.
- NAUMANN, A. W., G. J. SAFFORD, AND F. A. MUMPTON (1966) Low-frequency (OH) motions in layer silicate minerals. *Proc. Nat. Conf. Clays Clay Mineral.* **14**, 367–383.
- NODA, T., AND R. ROY (1956) OH-F exchange in fluorine phlogopite. *Amer. Mineral.* **41**, 929–932.
- , AND M. USHIO (1966) Hydrothermal synthesis of fluorine-hydroxyl-phlogopite. Part two: Relationship between the fluorine content, lattice constants, and the conditions of synthesis of fluorine-hydroxyl-phlogopite. *Collect. Pap. Syn. Crystal Res. Lab.*, Faculty of Eng., Nagoya Univ., Japan, No. **3**, 96–104.
- PAULING, L. (1930) The structure of micas and related minerals. *Proc. Nat. Acad. Sci.* **16**, 123–129.
- RADOSLOVICH, E. W. (1959) Structural control of polymorphism in micas. *Nature*, **183**, 253.
- ROSS, M. H., H. TAKEDA, AND D. R. WONES (1966) Mica polytypes: Systematic description and identification. *Science*, **151**, 191–193.
- ROTHBAUER, VON R. (1971) Untersuchung eines $2M_1$ -Muskovits mit neutronenstrahlen. *Neues Jahrb. Mineral. Monatsch.* **4**, 143–154.
- SADANAGA, R., AND U. TAKÉUCHI (1961) Polysynthetic twinning of micas. *Z. Kristallogr.* **116**, 406–429.
- STEINFINK, H. (1962) Crystal structure of a trioctahedral mica: Phlogopite. *Amer. Mineral.* **47**, 886–896.
- TAKEDA, H., AND C. W. BURNHAM (1969) Fluor-polyolithionite: a lithium mica with nearly hexagonal $(\text{Si}_2\text{O}_6)^{2-}$ ring. *Mineral. J. (Japan)* **6**, 102–109.
- TAKÉUCHI, Y. (1964) Structures of brittle micas. *Proc. Nat. Conf. Clays Clay Mineral.* **13**, 1–25.
- TOKONAMI, M. (1965) Atomic scattering factor for O^{2-} . *Acta Crystallogr.* **19**, 486.
- VEDDER, W., AND R. S. McDONALD (1963) Vibrations of the OH ions in muscovite. *J. Chem. Phys.* **38**, 1583–1590.
- YODER, H. S., AND H. P. EUGSTER (1955) Synthetic and natural muscovite. *Geochim. Cosmochim. Acta*, **8**, 225–280.

*Manuscript received, October 23, 1972;
accepted for publication, November 28, 1972.*